

A Spacetime Calculation of the Calabrese-Cardy Entanglement Entropy

Abhishek Mathur*, Sumati Surya and Nomaan X

Raman Research Institute, CV Raman Ave, Sadashivanagar, Bangalore, 560080, India

Abstract

We calculate Sorkin’s spacetime entanglement entropy of a Gaussian scalar field for complementary regions in the 2d cylinder spacetime and show that it has the Calabrese-Cardy form. We find that the cut-off dependent term is universal when we use a covariant UV cut-off as in [1]. In addition, we show that the relative size-dependent term exhibits complementarity. Its coefficient is however *not* universal and depends on the choice of pure state. It asymptotes to the universal form within a natural class of pure states.

The Calabrese-Cardy formula for the entanglement entropy (EE) of a CFT for an interval \mathcal{I}_s of length s in a circle \mathcal{C}_ℓ of circumference ℓ is given by

$$S = \frac{c}{3} \ln \left(\frac{\ell}{\pi \epsilon} \right) + \frac{c}{3} \ln(\sin(\alpha\pi)) + c_1 \quad (1)$$

where $\alpha = s/\ell$, c is the CFT central charge, ϵ is a UV cut-off and c_1 is a non-universal constant [2]. This formula has been shown to apply to a diverse range of two dimensional systems which fall within the same universality class, including a geometric realisation by Ryu and Takayanagi [3] and others [4]. Entanglement entropy (EE) was first proposed in [5] as a possible contributor to black hole entropy. Hence understanding Eqn. (1) from a spacetime perspective is of broad interest.

As a follow up to their earlier work, Calabrese and Cardy studied the unitary time evolution of the EE for an interval \mathcal{I}_s inside a larger interval $\mathcal{I} \supset \mathcal{I}_s$. Starting with a pure state, which is an eigenstate of a ”pre-quench” Hamiltonian, and then quenching the system at $t = 0$, they used path integral techniques to show that the EE increases with time. It then saturates after the ”light-crossing” time, in keeping with causality [6]. This corresponds to the ”time” required for the domain of dependence of \mathcal{I}_s to be fully defined. Seeking out a covariant formulation of EE is therefore of interest both to understanding the results of [6]

**abhishekmathur@rri.res.in*

in a spacetime language as well as more generally in QFT and quantum gravity. Such a formulation is moreover in keeping with the broader framework of AQFT, where observables are associated with spacetime regions rather than spatial hypersurfaces [7].

In [8] Sorkin proposed a spacetime formula for the EE of a Gaussian scalar field Φ in a globally hyperbolic subregion \mathcal{O} of a globally hyperbolic spacetime (M, g) , with respect to its causal complement \mathcal{O}^c . It uses the restriction of the Wightmann function $W(x, x')$ in M to \mathcal{O} , and the Pauli-Jordan function $i\Delta(x, x')$ which appears in the Peierl's spacetime commutation relation $[\hat{\Phi}(x), \hat{\Phi}(x')] = i\Delta(x, x')$.

Sorkin's spacetime EE (SSEE) of \mathcal{O} with respect to \mathcal{O}^c is

$$\mathcal{S} = \sum_{\mu} \mu \ln(|\mu|), \quad \widehat{W}|_{\mathcal{O}} \circ \chi = \mu(i\hat{\Delta}) \circ \chi, \quad (2)$$

where $\chi \notin \text{Ker}(\hat{\Delta})$ and where

$$A \circ v(x) \equiv \int_{\mathcal{O}} dV_{x'} A(x, x') v(x'). \quad (3)$$

It is motivated by the finite system Wightmann function for a Gaussian state which is a direct sum of identical systems with two degrees of freedom [8]. The SSEE formula generalises the calculation of EE for a state at a given time to that associated with a spacetime region.

In [1] the SSEE for nested causal diamonds $\mathcal{D}_s \subset \mathcal{D}_S$ was shown to yield the first, cut-off dependent term of Eqn. (1) with $c = 1$ when $s \ll S$. Since \mathcal{D}_s is the domain of dependence of \mathcal{I}_s , this is the natural spacetime analogue of $\mathcal{I}_s \subset \mathcal{I}_S$. In this work we calculate the SSEE for the spacetime analogue of $\mathcal{I}_s \subset \mathcal{C}_\ell$ for finite ℓ and additionally, find the same α -dependence as Eqn. (1), thus explicitly demonstrating complementarity. A natural spacetime analogue of \mathcal{C}_ℓ is its (zero momentum) Cauchy completion, which is the $d = 2$ cylindrical spacetime (M, g) with $ds^2 = -dt^2 + dx^2$, $x + \ell \sim x$. The domains of dependence of \mathcal{I}_s and its complement $\mathcal{I}_{\ell-s}$ in (M, g) are the causal diamonds \mathcal{D}_s and $\mathcal{D}_{\ell-s}$ respectively, as shown in Fig 1.

In what follows we use a mixture of analytical and numerical methods to solve the SSEE eigenvalue problem.

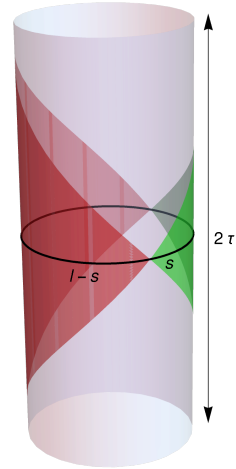


Figure 1: The spacetime analogues of $\mathcal{I}_s, \mathcal{I}_{\ell-s} \subset \mathcal{C}_\ell$ are their domains of dependence \mathcal{D}_s and $\mathcal{D}_{\ell-s}$ in (M, g) shown in green and red respectively.

We will find it convenient to work with the Sorkin-Johnston (SJ) formulation [9, 10, 11, 12, 13], where the SJ spectrum provides the required (covariant) UV cut-off with which to calculate \mathcal{S} , as was done in [1]. For a compact globally hyperbolic region (M, g) of a spacetime it follows from $\text{Ker}(\hat{\square}) = \text{Im}(i\hat{\Delta})$ [14] that the eigenmodes of the integral Hermitian operator $i\hat{\Delta}$ provide a covariant orthonormal basis (the SJ modes) with respect to the \mathcal{L}^2 norm on (M, g) [7]. The SJ vacuum or Wightmann function is given by the positive part of $i\hat{\Delta}$. Since the SJ spectrum is covariant so is a UV cut-off in this basis.

For our calculation of \mathcal{S} we will use the SJ vacuum W_τ for a free massless scalar field in a slab (M_τ, g) of height 2τ in the cylinder spacetime [10], and its restriction to $\mathcal{D}_s \subset M_\tau$,

$$W_\tau(x, t; x', t') = \sum_{m \in \mathbb{Z}} \varrho_m \psi_m(x, t) \psi_m^*(x', t'), \quad (4)$$

where $\{\psi_m, \varrho_m\}$ are the \mathcal{L}^2 normalised positive frequency SJ eigenmodes and eigenvalues in M_τ [10]:

$$\begin{aligned} \psi_m(x, t) &= \left(\frac{(1 - \zeta_m)}{2\sqrt{2\ell}c_m} e^{i\frac{2\pi|m|t}{\ell}} + \frac{(1 + \zeta_m)}{2\sqrt{2\ell}c_m} e^{-i\frac{2\pi|m|t}{\ell}} \right) e^{i\frac{2\pi mx}{\ell}} \\ \varrho_m &= \ell \frac{s_m c_m}{2\pi|m|}, \quad \zeta_m = \frac{c_m}{s_m}, \quad \gamma = \frac{2\tau}{\ell}, \quad m \in \mathbb{Z}, \\ c_m^2 &= \tau (1 + \text{sinc}(2|m|\pi\gamma)), \quad s_m^2 = \tau (1 - \text{sinc}(2|m|\pi\gamma)). \end{aligned} \quad (5)$$

The $m = 0$ “zero mode” in particular takes the form

$$\psi_0(t) = \frac{1}{2\sqrt{\tau\ell}} \left(1 - i \frac{\sqrt{3}}{\tau} t \right), \quad \varrho_0 = \frac{2}{\sqrt{3}} \tau^2. \quad (6)$$

Unlike the standard vacuum on the cylinder, W_τ is τ -dependent. Each W_τ can however be viewed as a pure (non-vacuum) state in $M_{\bar{\tau}}$ for any $\bar{\tau} > \tau$, as we will later show. To accommodate both \mathcal{D}_s and $\mathcal{D}_{\ell-s}$ in our calculations, we require $2\tau \geq s, \ell - s$.

The SJ modes in \mathcal{D}_s are naturally expressed in terms of the light cone coordinates $u = \frac{1}{\sqrt{2}}(t - x), v = \frac{1}{\sqrt{2}}(t + x)$ and come in the two mutually orthogonal series [15]

$$\begin{aligned} f_k &= e^{-iku} - e^{-ikv}, \quad k = 2\sqrt{2}n\pi/s \\ g_\kappa &= e^{-i\kappa u} + e^{-i\kappa v} - 2 \cos\left(\frac{\kappa s}{2\sqrt{2}}\right), \quad \tan\left(\frac{\kappa s}{2\sqrt{2}}\right) = \frac{\kappa s}{\sqrt{2}} \end{aligned} \quad (7)$$

with eigenvalues $\lambda_k = \frac{s}{2\sqrt{2}k}$ and $\lambda_\kappa = \frac{s}{2\sqrt{2}\kappa}$, respectively, and with \mathcal{L}^2 norm in \mathcal{D}_s

$$\|f_k\|^2 = s^2, \quad \|g_\kappa\|^2 = s^2 \left(1 - 2 \cos^2\left(\frac{\kappa s}{2\sqrt{2}}\right) \right). \quad (8)$$

Since $i\widehat{\Delta}$ is diagonal in this basis we will use it to transform Eqn. (2) to the matrix form

$$\widehat{W}_\tau|_{\mathcal{D}_s} X = \mu \Lambda X, \quad (9)$$

where Λ is the diagonal matrix $\{\lambda_k, \lambda_\kappa\}$. For $X \notin \text{Ker}(i\widehat{\Delta})$, we can invert this to suggestively write

$$\widehat{\rho} X = \Lambda^{-1} \widehat{W}_\tau|_{\mathcal{D}_s} X = \mu X, \quad (10)$$

so that \mathcal{S} can be viewed as the von-Neumann entropy of $\widehat{\rho}$. The spectrum of $\widehat{\rho}$ is unbounded and hence needs a UV cut-off. As in [1] we use the covariant UV-cut off with respect to the SJ spectrum $\{\lambda_k, \lambda_\kappa\}$. For large κ the condition $\tan(\kappa s/2\sqrt{2}) = \kappa s/\sqrt{2}$ can be approximated by $\kappa \sim \sqrt{2}(2n+1)\pi/s$, so that a consistent choice of cut-off for both sets of eigenvalues is $\epsilon = k_{\text{max}}^{-1} = s/(2\sqrt{2}n_{\text{max}}\pi)$. We also need to ensure that this same cut-off is used in the causal complement, i.e., $k_{\text{max}} = 2\sqrt{2}n'_{\text{max}}\pi/(\ell - s)$, where n' denotes the quantum number for the SJ spectrum in $\mathcal{D}_{\ell-s}$, so that $\epsilon = \frac{\ell\alpha}{2\sqrt{2}\pi n_{\text{max}}} = \frac{\ell(1-\alpha)}{2\sqrt{2}\pi n'_{\text{max}}}$.

We expand the SJ modes in M_τ in terms of those in \mathcal{D}_s to obtain the non-zero matrix elements for $\widehat{W}_\tau|_{\mathcal{D}_s}$ for general α, γ . Suppressing the τ, \mathcal{D}_s labels, these are

$$\begin{aligned} \widehat{W}_{kk'} &= \frac{s^4}{32\pi} \sum_{m>0} \frac{1}{|m|\zeta_m} \left(\eta_m^- \text{sinc}(x_+) - \eta_m^+ \text{sinc}(x_-) \right) \times \left(\eta_m^- \text{sinc}(x'_+) - \eta_m^+ \text{sinc}(x'_-) \right) \\ \widehat{W}_{\kappa\kappa'} &= \frac{s^4}{32\pi} \sum_{m>0} \frac{1}{|m|\zeta_m} \left(\eta_m^- \text{sinc}(z_+) + \eta_m^+ \text{sinc}(z_-) \right) \times \left(\eta_m^- \text{sinc}(z'_+) + \eta_m^+ \text{sinc}(z'_-) \right) \\ &\quad + \widehat{W}_{\kappa\kappa'}^{(0)} \end{aligned} \quad (11)$$

where $x_\pm = (n \pm \alpha m)\pi$, $x'_\pm = (n' \pm \alpha m)\pi$, $z_\pm = \kappa s/2\sqrt{2} \pm \alpha m\pi$, $z'_\pm = \kappa' s/2\sqrt{2} \pm \alpha m\pi$, and the contribution from the zero mode is

$$\begin{aligned} \widehat{W}_{\kappa\kappa'}^{(0)} &= \frac{s^4}{2\sqrt{3}} \frac{\tau}{\ell} \cos(\kappa s/(2\sqrt{2})) \cos(\kappa' s/(2\sqrt{2})) \\ &\quad \times \left(1 + \sqrt{\frac{3}{2}} \frac{1}{\kappa\tau} \right) \left(1 + \sqrt{\frac{3}{2}} \frac{1}{\kappa'\tau} \right). \end{aligned} \quad (12)$$

Our strategy is to construct $\widehat{\rho}$ from these matrix elements and to solve for its eigenvalues using a numerical matrix solver. However, each matrix elements in Eqn. (11) is an infinite sum over the quantum number m and hence not amenable to explicit calculation. We therefore need to find a closed form expression for the above matrix elements.

We notice that when γ takes half-integer values (for which the SJ vacuum Hadamard [10]), $\zeta_m = 1$ for $m \neq 0$, which leads to a considerable simplification. Further, let α be rational, so that we can write $\alpha = \frac{p}{q}$, with $p, q \in \mathbb{Z}$, and $p, q > 0$ being relatively prime. For these choices of α and γ , the infinite sums of Eqn. (11) reduce to the following finite sums over Polygamma functions $\Psi(x)$ and $\Psi^{(1)}(x)$

$$\begin{aligned}
\widehat{W}_{kk'} &= \frac{s^4}{8\pi n} \left[\delta_{n,n'} \left(\alpha \Theta(n) \sum_m \delta_{n,m\alpha} + \frac{1}{\pi^2 \alpha q^2 n} \sum_{r=1}^{q-1} \sin^2(r\alpha\pi) \left[-\alpha q \Psi\left(\frac{r}{q}\right) + \alpha q \Psi\left(\frac{\alpha r - n}{\alpha q}\right) \right. \right. \right. \\
&\quad \left. \left. \left. + n \Psi^{(1)}\left(\frac{\alpha r - n}{\alpha q}\right) \right] \right) + (1 - \delta_{n,n'}) \frac{(-1)^{n+n'}}{\pi^2 n' (n - n') q} \sum_{r=1}^{q-1} \sin^2(r\alpha\pi) \left[(n' - n) \Psi\left(\frac{r}{q}\right) \right. \right. \\
&\quad \left. \left. - n' \Psi\left(\frac{\alpha r - n}{\alpha q}\right) + n \Psi\left(\frac{\alpha r - n'}{\alpha q}\right) \right] \right] \\
\widehat{W}_{\kappa\kappa'} &= s^4 \cos\left(\frac{\kappa s}{2\sqrt{2}}\right) \cos\left(\frac{\kappa' s}{2\sqrt{2}}\right) \left[\frac{\tau}{2\sqrt{3}\ell} \left(1 + \sqrt{\frac{3}{2}} \frac{1}{\tau\kappa}\right) \left(1 + \sqrt{\frac{3}{2}} \frac{1}{\tau\kappa'}\right) \right. \\
&\quad \left. + \delta_{\kappa,\kappa'} \frac{1}{\alpha q^2 s^2 \kappa^2 \pi^2} \left(\sum_{r=1}^{q-1} \Omega(\kappa, \kappa', \alpha, r) \left[\alpha q \pi \left(\Psi\left(\frac{r}{q} - \frac{\kappa s}{\eta}\right) - \Psi\left(\frac{r}{q}\right) \right) + \frac{\kappa s}{2\sqrt{2}} \Psi^{(1)}\left(\frac{r}{q} - \frac{\kappa s}{\eta}\right) \right] \right. \right. \\
&\quad \left. \left. + \frac{s^2 \kappa \kappa'}{2} \left[\alpha q \pi \left(\gamma_e + \Psi\left(1 - \frac{\kappa s}{\eta}\right) \right) + \frac{\kappa s}{2\sqrt{2}} \Psi^{(1)}\left(1 - \frac{\kappa s}{\eta}\right) \right] \right) + (1 - \delta_{\kappa,\kappa'}) \frac{1}{s^2 q \kappa \kappa' (\kappa - \kappa')} \right. \\
&\quad \times \left(\sum_{r=1}^{q-1} \Omega(\kappa, \kappa', \alpha, r) \left[\kappa \Psi\left(\frac{r}{q} - \frac{\kappa' s}{\eta}\right) - \kappa' \Psi\left(\frac{r}{q} - \frac{\kappa s}{\eta}\right) - (\kappa - \kappa') \Psi\left(\frac{r}{q}\right) \right] \right. \\
&\quad \left. \left. + \frac{s^2 \kappa \kappa'}{2} \left[\gamma_e (\kappa - \kappa') + \kappa \Psi\left(1 - \frac{\kappa' s}{\eta}\right) - \kappa' \Psi\left(1 - \frac{\kappa s}{\eta}\right) \right] \right) \right], \quad \eta = 2\sqrt{2} \alpha q \pi \quad (13)
\end{aligned}$$

where γ_e represents the Euler-Mascheroni constant and

$$\begin{aligned}
\Omega(\kappa, \kappa', \alpha, r) &= \kappa \kappa' \frac{s^2}{2} \cos^2(\alpha r \pi) + \sin^2(\alpha r \pi) \\
&\quad - (\kappa + \kappa') \frac{s}{2\sqrt{2}} \sin(2\alpha r \pi). \quad (14)
\end{aligned}$$

We are now in a position to solve for the eigenvalues of $\widehat{\rho}$ using Mathematica's numerical eigenvalue solver. We consider a range of values of α, γ and the cut-off n_{\max}/α given in the table below.

α	$\frac{1}{10}, \frac{1}{5}, \frac{1}{4}, \frac{1}{3}, \frac{1}{2}, \frac{2}{3}, \frac{3}{4}, \frac{4}{5}, \frac{9}{10}$
γ	1, 2, 4, 6, 8, 16, 21.5, 32, 40.3, 100, 200, 1000, 2000
$\frac{n_{\max}}{\alpha}$	1000, 1200, 1400, 1600, 1800, 2000, 2200, 2400, 2600

In the list of γ values, we have also included the specific non-half-integer value of $\gamma = 40.3$ for which $\zeta_m \sim 1$ even for $m = 1$. In general, we note that $\zeta_m \sim 1$ for $m \gg \gamma^{-1}$. The

error coming from small m terms has been explicitly calculated in this case as a function of m and seen to be small. For the special case $\alpha = 0$, \mathcal{S} is trivially zero, while for $\alpha = 1$, the domain of dependence of \mathcal{C}_ℓ is no longer a causal diamond, but all of M_τ . Since \widehat{W}_τ is the SJ vacuum and therefore pure, $\mathcal{S} = 0$.

Fig. 2 shows the results of simulations for these various α and γ values, for a fixed choice of cut-off $n_{\max}/\alpha = 2600$. It is already clear that \mathcal{S} satisfies complementarity. This is much more explicit in Fig. 3, where we vary over the cut-off. Our numerical results suggest that

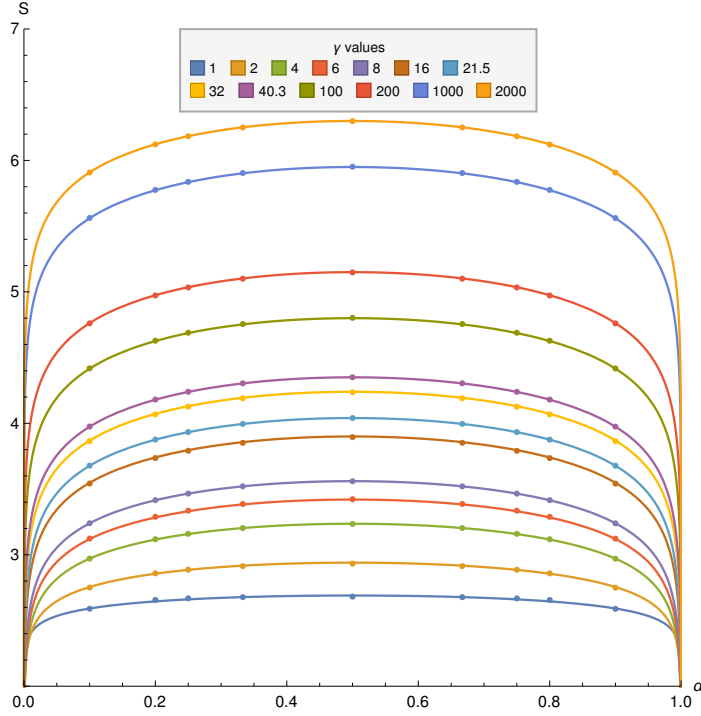


Figure 2: \mathcal{S} vs α for different γ fitted to $\mathcal{S} = a \log(\sin(\pi\alpha)) + b$, with $\frac{n_{\max}}{\alpha} = 2600$.

\mathcal{S} takes the general form

$$\mathcal{S} = \frac{c(\gamma)}{3} \ln \left(\frac{\ell}{\pi\epsilon} \right) + f(\gamma) \ln(\sin(\alpha\pi)) + c_1(\gamma). \quad (15)$$

Using the best-fit curves in Figs. 3-5, and the associated data in the appendix, we find that $c(\gamma) \sim 1$ and

$$\begin{aligned} f(\gamma) &\sim 0.33 + a/\gamma + b/\gamma^2 \\ c_1(\gamma) &\sim a' \log \gamma + b'. \end{aligned} \quad (16)$$

Thus, the first term of Eqn. (1) is reproduced for any choice of α, γ . This generalises the results of [1] where this was shown in the limit of $\alpha \ll 1$. The dependence on α , i.e.,

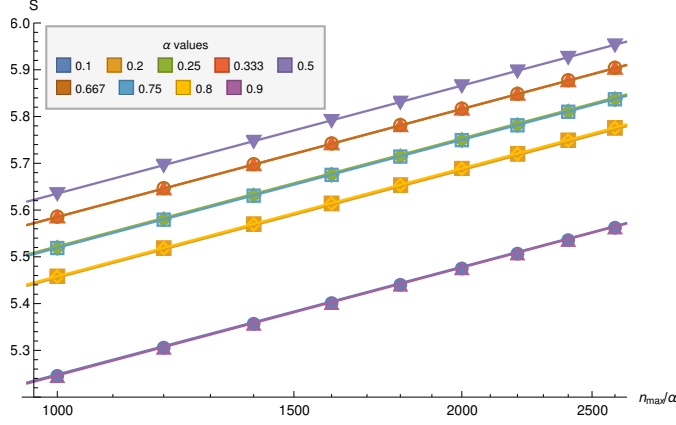


Figure 3: Log-linear plot of \mathcal{S} vs $\frac{n_{\max}}{\alpha}$ for different α fitted to $\mathcal{S} = a \log(n_{\max}/\alpha) + b$ for $\gamma = 1000$.

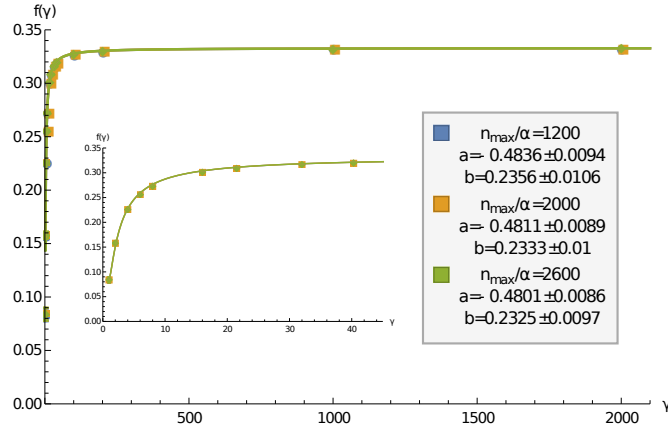


Figure 4: A plot of $f(\gamma)$ vs. γ for different values of n_{\max}/α , fitted to $0.33 + a/\gamma + b/\gamma^2$. The inset figure shows the smaller γ values.

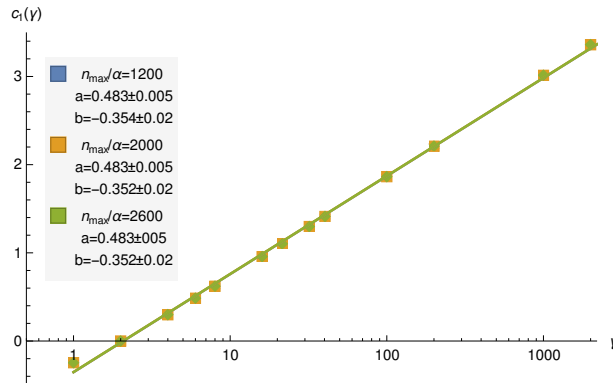


Figure 5: A log-linear plot of $c_1(\gamma)$ vs γ for different values of n_{\max}/α fitted to $a \log \gamma + b$.

the second term of Eqn. (1) is also reproduced and hence exhibits complementarity for any α (see Fig. 2, 3). Its coefficient however is *not* universal and depends on γ as shown in Fig. 4. However, as $\gamma \gg 1$, $f(\gamma)$ does asymptote to the universal value $1/3$. Finally, the non-universal constant $c_1(\gamma)$ diverges logarithmically with γ as shown in Fig. 5. This can be traced to the IR divergence in the zero modes of the massless theory.

The behaviour of $f(\gamma)$ can be viewed as a dependence on the choice of the pure state W_τ in $M_{\bar{\tau}}$, for $M_{\bar{\tau}} \supset M_\tau$. From Eqn. (4) we see that \widehat{W}_τ is a state in $M_{\bar{\tau}}$, i.e., $\widehat{W}_\tau = \widehat{R}_\tau + i\widehat{\Delta}/2$, where \widehat{R}_τ is real and symmetric.

Expanding $i\widehat{\Delta}$ in the SJ modes $\{\psi_m^{(\bar{\tau})}\}$ of $M_{\bar{\tau}}$ and \widehat{W}_τ in $\{\psi_m^{(\tau)}\}$, and inserting in Eqn. (2) we see that term by term

$$\varrho_m^\tau \psi_m^{(\tau)}(x, t) A_m = \mu \varrho_m^{\bar{\tau}} [\psi_m^{(\bar{\tau})}(t, x) \bar{A}_m - \psi_m^{*(\bar{\tau})}(t, x) \bar{B}_m],$$

where $A_m = (\psi_m^{(\tau)}, \chi)_{\bar{\tau}}$, $\bar{A}_m = (\psi_m^{(\bar{\tau})}, \chi)_{\bar{\tau}}$, $\bar{B}_m = (\psi_m^{*(\bar{\tau})}, \chi)_{\bar{\tau}}$ and $(\cdot, \cdot)_{\bar{\tau}}$ is the \mathcal{L}^2 inner product in $M_{\bar{\tau}}$. Expanding $\psi_m^{(\tau)} = a_m \psi_m^{(\bar{\tau})} + b_m \psi_m^{*(\bar{\tau})}$, $a_m = \frac{s_m^{\tau'}}{2c_m^{\tau'}} (\zeta_m^{(\tau')} + \zeta_m^{(\tau)})$, $b_m = \frac{s_m^{\tau'}}{2c_m^{\tau'}} (\zeta_m^{(\tau')} - \zeta_m^{(\tau)})$ this simplifies to

$$\begin{aligned} \varrho_m^\tau a_m (a_m \bar{A}_m + b_m \bar{B}_m) &= \mu \varrho_m^{\bar{\tau}} \bar{A}_m \\ \varrho_m^\tau b_m (a_m \bar{A}_m + b_m \bar{B}_m) &= -\mu \varrho_m^{\bar{\tau}} \bar{B}_m. \end{aligned} \quad (17)$$

The solutions for this are either $a_m \bar{A}_m + b_m \bar{B}_m = 0 \Rightarrow \mu = 0$, or $a_m \bar{B}_m + b_m \bar{A}_m = 0 \Rightarrow \mu = \frac{\varrho_m^\tau}{\varrho_m^{\bar{\tau}}} (a_m^2 - b_m^2) = 1$, which means that \widehat{W}_τ is a pure state in $M_{\bar{\tau}}$. Thus $f(\gamma)$ can be viewed as the dependence on the choice of pure state in $M_{\bar{\tau}}$ for $M_\tau \subset M_{\bar{\tau}}$.

We end with some remarks. While we have demonstrated complementarity for certain rational values of α , an analytic demonstration using Eqn. (13) seems non-trivial, in part because the UV regulated matrices $\widehat{\rho}_\alpha$ and $\widehat{\rho}_{1-\alpha}$ are of different dimensions. Conversely, complementarity implies that if $n_{\max} > n'_{\max}$, $\widehat{\rho}_\alpha = \widehat{\rho}_{1-\alpha} \oplus \mathbf{1}_N \oplus \mathbf{0}_N$, where $\mathbf{0}$ is the zero matrix and $N = (n_{\max} - n'_{\max})/2$.

In our computations we find that the eigenvalues of $\widehat{\rho}$ (which always come in pairs $(\mu, 1 - \mu)$) exhibit the surprising feature that all but one pair hovers around the values 0 and 1, thus contributing most significantly to \mathcal{S} . Indeed, the \mathcal{S} calculated using the largest few pairs of eigenvalues accounts for most of the entropy (see appendix).

Finally, it would be interesting to calculate the non-zero mass case which is IR divergence free. While the small mass approximation of the SJ modes in \mathcal{D}_s is known [16], the challenge will be to obtain closed form expressions for the matrix elements of \widehat{W} as we have done.

Acknowledgements

SS is supported in part by a Visiting Fellowship at the Perimeter Institute. Research at Perimeter Institute is supported in part by the Government of Canada through the Depart-

ment of Innovation, Science and Economic Development Canada and by the Province of Ontario through the Ministry of Colleges and Universities.

Appendix: Supporting Data

In this appendix we present some plots with additional data which were used to compute the coefficients $c(\gamma)$, $f(\gamma)$ and $c_1(\gamma)$ in the Entanglement Entropy.

Fig. 6 shows the dependence of \mathcal{S} on α for different values of γ and with three different values of n_{max}/α (1200, 2000 and 2600). The SSEE can be fitted to the form $\mathcal{S} = a_1 \log(\sin(\alpha\pi)) + b_1$ where the coefficient a_1 corresponds to $f(\gamma)$ in Eqn. (15). The values of a_1 and b_1 along with their errors are given in the tables in Fig. 6. a_1 and therefore $f(\gamma)$ can be seen to be independent of n_{max}/α . It is however dependent on γ and asymptotes to the universal value of $1/3$ in the Calabrese-Cardy formula for $\gamma \gg 1$. We fit $f(\gamma)$ values to the form

$$f(\gamma) = 0.33 + a_2/\gamma + b_2/\gamma^2 \quad (18)$$

and find the $a_2 \approx -0.48$ and $b_2 \approx 0.23$ with the error given in the tables of Fig. 4.

Fig. 7 shows the dependence of \mathcal{S} on n_{max}/α for different α and with three different values of γ (16, 200 and 1000). Here SSEE can be fitted to the form, $\mathcal{S} = a_3 \log(n_{max}/\alpha) + b_3$. As is clear from the tables in this figure $a_3 \approx 0.33 \approx 1/3$ for all α and γ with the order of error given in the table. b_3 however depends on α and γ . This suggests that $c(\gamma) \approx 1$ in Eqn. (15).

In order to extract $c_1(\gamma)$ we subtract the first term in Eqn. (15) (which depends on n_{max}/α) using $c(\gamma)/3$ given by the values of a_3 in the table of Fig. 7 from the values of b_1 in the table of Fig. 6 for $n_{max}/\alpha = 1200, 2000$ and 2600 . We find that the difference (or $c_1(\gamma)$) is independent of the choice of n_{max}/α which is as expected. We fit the dependence on γ by

$$c_1(\gamma) = a_4 \log(\gamma) + b_4 \quad (19)$$

and the values for the coefficients are given in the table in the Fig. 5.

We also find that the eigenvalues (which always come in pairs $(\mu, 1 - \mu)$) exhibit the surprising feature that all but one pair hovers around the values 0 and 1 and hence contributes significantly to \mathcal{S} . In Fig. 8 we also show the comparison of the eigenvalues obtained in the two complementary regions, we find that they differ only in the numbers of $(0, 1)$ pairs. Further, if we calculate \mathcal{S} for the largest pairs of eigenvalues, we find that the error is small, as shown in Fig 9.

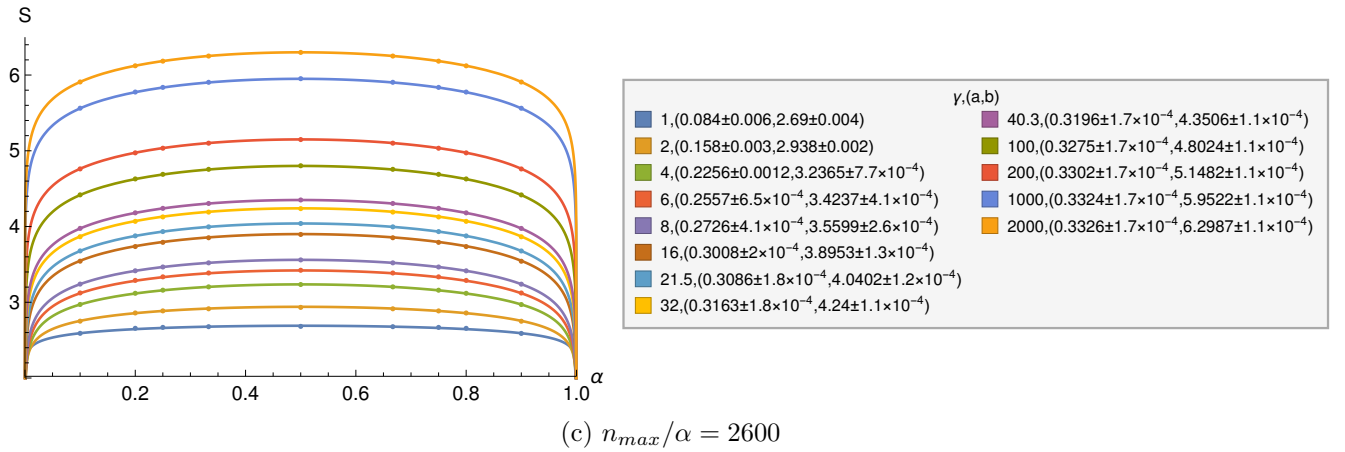
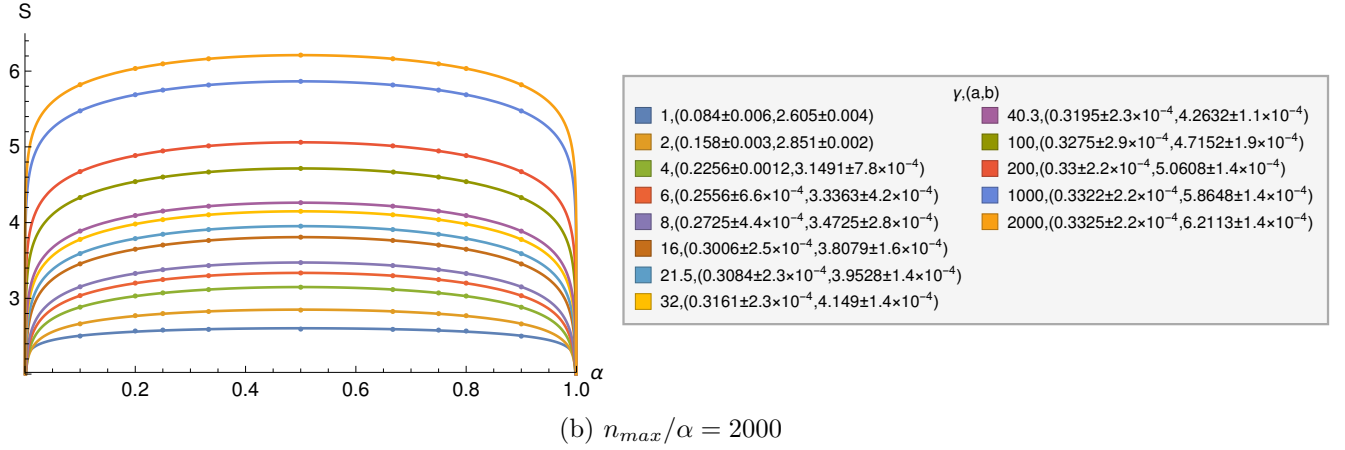
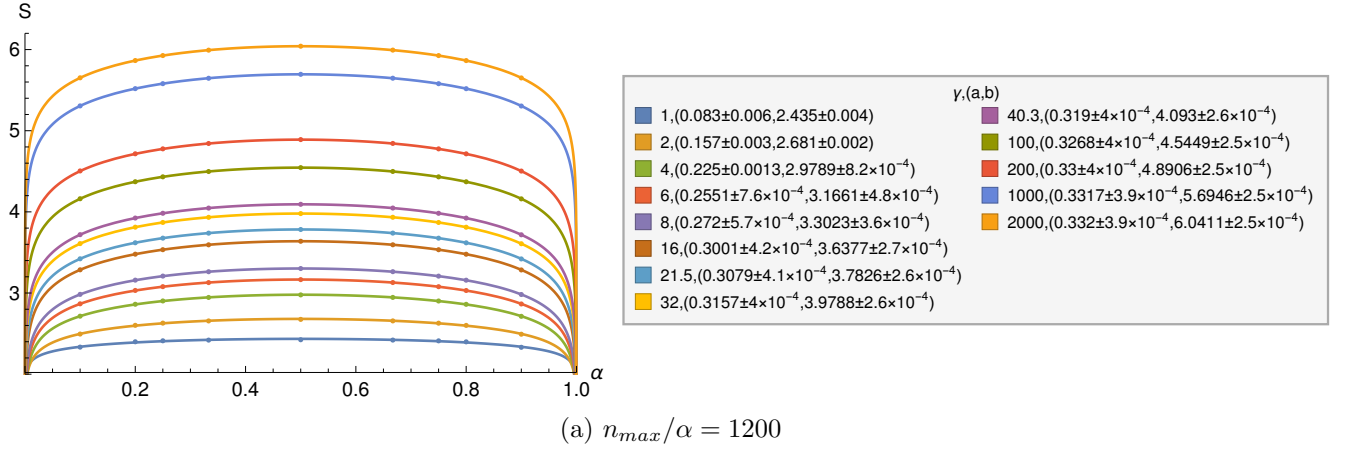
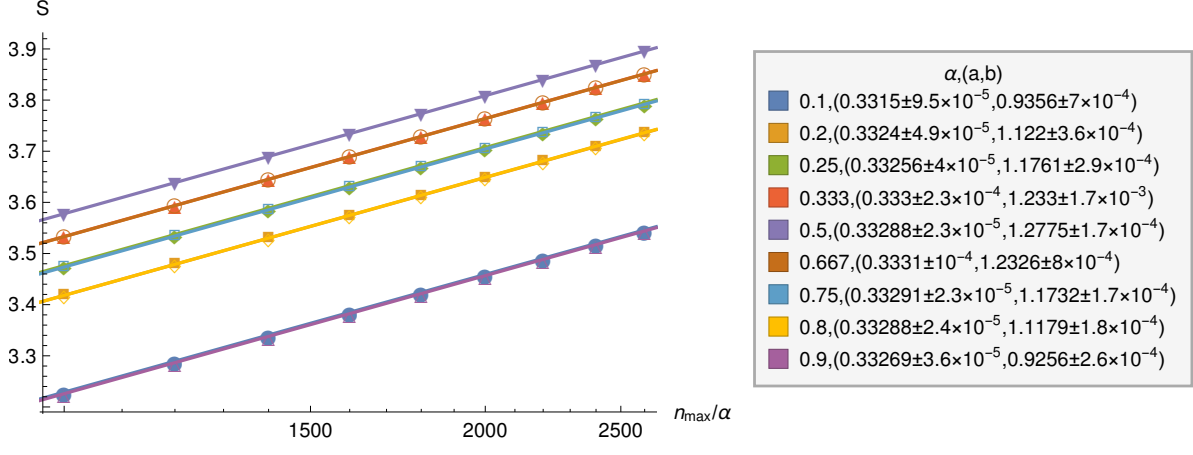
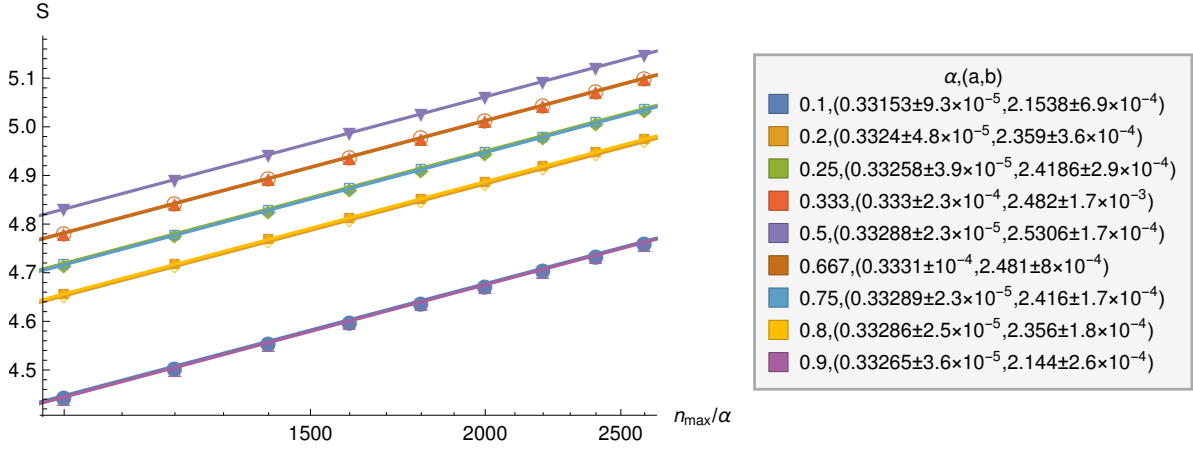


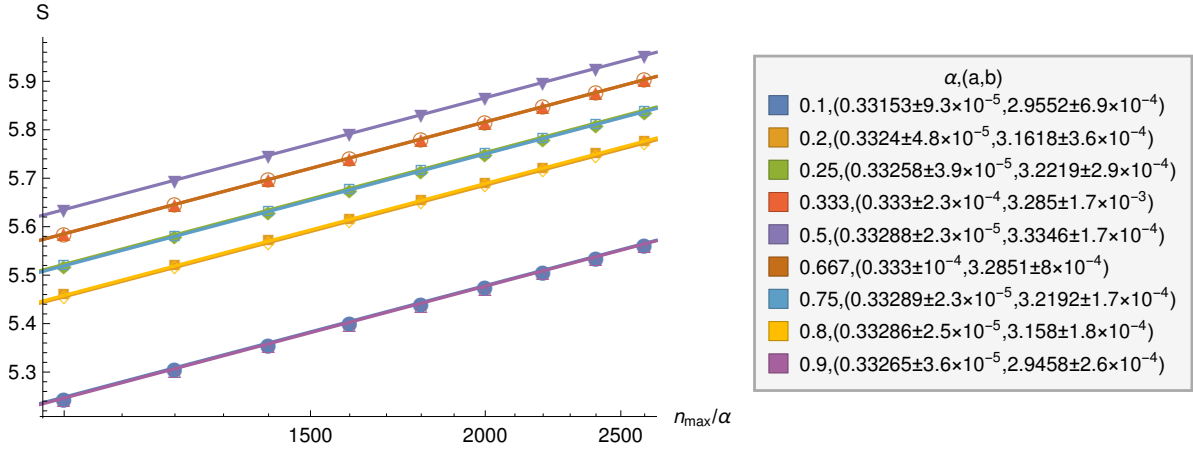
Figure 6: \mathcal{S} vs α for different γ with $n_{\max}/\alpha = 1200, 2000$ and 2600 fitted to $\mathcal{S} = a \log(\sin(\pi\alpha)) + b$. The fit parameters are shown in the table.



(a) $\gamma = 16$



(b) $\gamma = 200$



(c) $\gamma = 1000$

Figure 7: A log-linear plot of \mathcal{S} vs n_{\max}/α for different α with $\gamma = 16, 200$ and 1000 fitted to $\mathcal{S} = a \log(n_{\max}/\alpha) + b$. The fit parameters are shown in the table which show $a \sim 1/3$. This is also true for other values of γ . The curves for complementary values of α are indistinguishable.

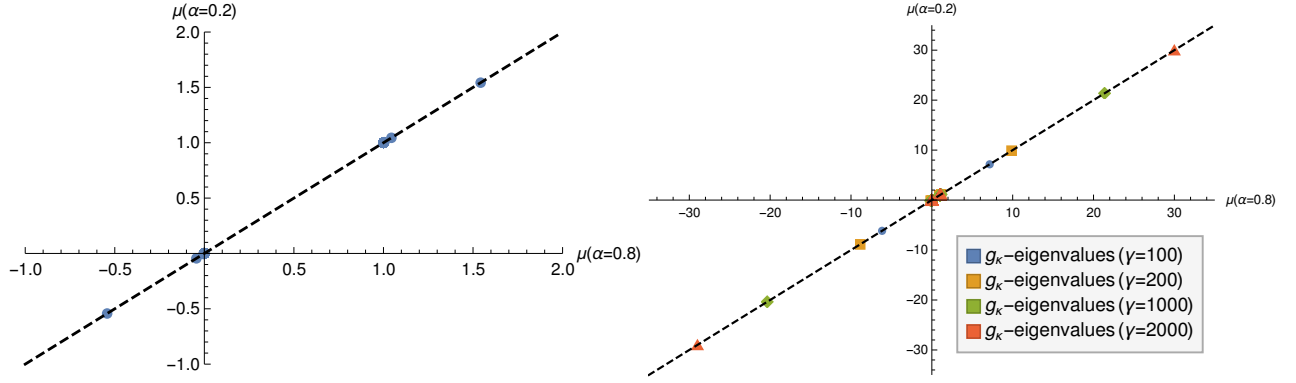


Figure 8: A plot comparing the eigenvalues μ of the entropy equation for one choice of complementary regions with $\alpha = 0.2, 0.8$ for $n_{\max}/\alpha = 2600$ and different choices of γ . On the left are the eigenvalues associated with the f_k matrix elements which are independent of γ and on the right are those associated with the g_k , which are γ dependent. We note that the number of eigenvalues differ in both regions but only in the number of $(1, 0)$ pairs which leads to the equality of the SSEE in these complementary regions. Further, the significant contribution comes from the g_k matrix elements of which there are precisely *two* which are substantially different from $(1, 0)$. These increase with γ and are the main contributors to $c_1(\gamma)$

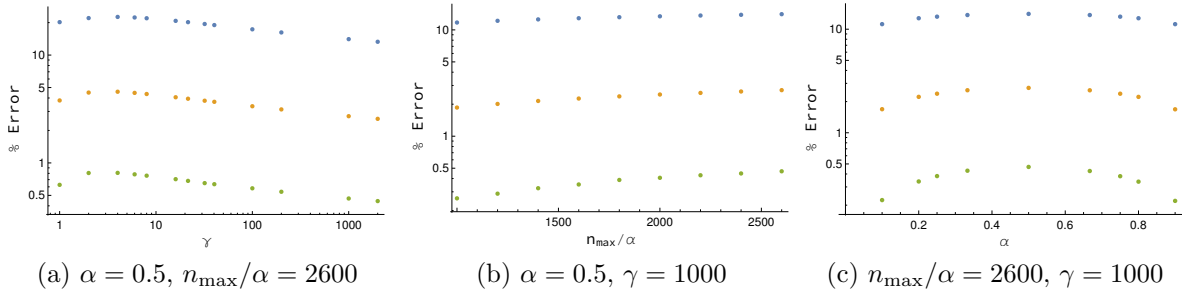


Figure 9: In order to estimate the contribution of the pairs $(\mu, 1 - \mu)$, we plot the percentage error in the SSEE when only the largest pairs (one, two and three represented in blue, orange and green respectively) of eigenvalues are considered, as a function of the different parameters $\gamma, n_{\max}/\alpha$ and α . In each case, we see that the error goes down to $< 1\%$ even when only the 3 largest eigenvalues are retained.

References

- [1] M. Saravani, R. D. Sorkin, and Y. K. Yazdi, “Spacetime entanglement entropy in 1 + 1 dimensions,” *Class. Quant. Grav.*, vol. 31, no. 21, p. 214006, 2014.
- [2] P. Calabrese and J. L. Cardy, “Entanglement entropy and quantum field theory,” *J. Stat. Mech.*, vol. 0406, p. P06002, 2004.

- [3] S. Ryu and T. Takayanagi, “Holographic derivation of entanglement entropy from the anti-de sitter space/conformal field theory correspondence,” *Physical review letters*, vol. 96, no. 18, p. 181602, 2006.
- [4] M. Headrick, “Lectures on entanglement entropy in field theory and holography,” *arXiv preprint arXiv:1907.08126*, 2019.
- [5] L. Bombelli, R. K. Koul, J. Lee, and R. D. Sorkin, “A Quantum Source of Entropy for Black Holes,” *Phys. Rev.*, vol. D34, pp. 373–383, 1986.
- [6] P. Calabrese and J. L. Cardy, “Evolution of entanglement entropy in one-dimensional systems,” *J. Stat. Mech.*, vol. 0504, p. P04010, 2005.
- [7] C. J. Fewster and K. Rejzner, “Algebraic quantum field theory,” in *Progress and Visions in Quantum Theory in View of Gravity*, pp. 1–61, Springer, 2020.
- [8] R. D. Sorkin, “Expressing entropy globally in terms of (4D) field-correlations,” *J. Phys. Conf. Ser.*, vol. 484, p. 012004, 2014.
- [9] R. D. Sorkin, “From Green Function to Quantum Field,” *Int. J. Geom. Meth. Mod. Phys.*, vol. 14, no. 08, p. 1740007, 2017.
- [10] C. J. Fewster and R. Verch, “On a Recent Construction of ‘Vacuum-like’ Quantum Field States in Curved Spacetime,” *Class. Quant. Grav.*, vol. 29, p. 205017, 2012.
- [11] M. Brum and K. Fredenhagen, “‘Vacuum-like’ Hadamard states for quantum fields on curved spacetimes,” *Class. Quant. Grav.*, vol. 31, p. 025024, 2014.
- [12] N. Afshordi, S. Aslanbeigi, and R. D. Sorkin, “A distinguished vacuum state for a quantum field in a curved spacetime: formalism, features, and cosmology,” *Journal of High Energy Physics*, vol. 2012, no. 8, p. 137, 2012.
- [13] N. Afshordi, M. Buck, F. Dowker, D. Rideout, R. D. Sorkin, and Y. K. Yazdi, “A Ground State for the Causal Diamond in 2 Dimensions,” *JHEP*, vol. 10, p. 088, 2012.
- [14] R. M. Wald, *Quantum field theory in curved spacetime and black hole thermodynamics*. University of Chicago press, 1994.
- [15] S. P. Johnston, *Quantum Fields on Causal Sets*. PhD thesis, Imperial Coll., London, 2010.
- [16] A. Mathur and S. Surya, “Sorkin-Johnston vacuum for a massive scalar field in the 2D causal diamond,” *Phys. Rev. D*, vol. 100, no. 4, p. 045007, 2019.